J. Membrane Biol. 188, 237–248 (2002)
DOI: 10.1007/s00232-001-0187-x

The Journal of
Membrane
Biology

The Phytotoxic Lipodepsipeptide Syringopeptin 25A from *Pseudomonas syringae* pv *syringae* Forms Ion Channels in Sugar Beet Vacuoles

A. Carpaneto[1], M. Dalla Serra[2], G. Menestrina[2], V. Fogliano[3], F. Gambale[1]
[1]CNR, Istituto di Biofisica, Via de Marini 6, 16149 Genova, Italy
[2]ITC-CNR IBF, Centro di Fisica degli Stati Aggregati, 38050 Povo (Trento), Italy
[3]Dipartimento di Scienza degli Alimenti, Università di Napoli Federico II, 80138 Napoli, Italy

Received: 15 February 2002/Revised: 26 April 2002

Abstract. Syringopeptin 25A ($SP_{25}A$) belongs to a family of cyclic lipodepsipeptides (LDPs) produced by the gram-negative bacterium *Pseudomonas syringae*, a phytopathogenic organism that affects several plants of agronomic interest. LDPs increase the permeability of plasma and, possibly, intracellular membranes in plant cells. Consistently, $SP_{25}A$ forms ion channels in planar lipid bilayers and other model membranes. Here we used sugar beet tonoplasts as a new biological model system to study toxin action. When applied to the vacuoles by a fast perfusion procedure, $SP_{25}A$ increases membrane permeability by forming discrete ion channels even at low applied potentials. The $SP_{25}A$ channel displays anion selectivity (with a Cl^-/K^+ permeability ratio of 6.7 ± 1.3) and has intrinsic rectification properties that derive from a different channel conductance at negative and positive voltages, presumably owing to an asymmetric distribution of fixed charges on the pore. Substitution of chloride with different anions reveals the following selectivity sequence $NO_3^- \approx Cl^- > F^- >$ gluconate$^-$, suggesting that the permeation pore is filled with water. The properties of the $SP_{25}A$ channels in vacuolar membranes are similar to those observed in planar lipid membranes prepared with asolectin. This work provides a direct demonstration of toxin effects on a native plant membrane, extending to a biological system previous results obtained on artificial planar lipid membranes.

Key words: Ion channels — Patch clamp — Anion selectivity

Introduction

Syringopeptin 25A ($SP_{25}A$) is a lipodepsipeptide (LDP) produced by the plant pathogen *Pseudomonas syringae* pv. *syringae* (Bradbury, 1986; Ballio et al., 1991). It is composed of two parts (*see* Fig. 1*D*): a peptide moiety of 25 amino acids with a cyclic ring of 8 amino acids at the C-terminus and a long unbranched 3-hydroxy fatty acid chain attached at the C-terminus of the peptide chain. $SP_{25}A$ is a basic molecule since the cyclic ring contains two positively charged residues (2,4-diaminobutanoic acid) (Ballio et al., 1991; Isogai et al., 1995). The three-dimensional structure of $SP_{25}A$ in aqueous solution, obtained by the interpretation of its two-dimensional NMR spectra (Ballio et al., 1995), is characterized by three structural regions: a loop including residues from Pro2 to Val6, a helicoidal zone (close to a left-handed alpha helix) including residues from Ala8 to Ala15, and a large lactone ring including residues from Thr18 to Tyr25. The type of ring conformation is the same found in two other bioactive lipodepsinonapeptides, the white line-inducing principle (WLIP) produced by *P. reactans* (Mortishire-Smith et al., 1991; Han et al., 1992) and siringotoxin produced by *P. syringae* pv. *syringae* (Ballio et al., 1990), and resembles the seam of a tennis ball. Its marked phytotoxic activity (Iacobellis et al., 1992; Di Giorgio, Camoni & Ballio, 1994; Di Giorgio et al., 1996a; 1996b) indicates that $SP_{25}A$ may give a significant contribution to the virulence activity of *P. syringae*,

Correspondence to: A. Carpaneto, email: carpanet@icb.ge.cnr.it

Abbreviations: $SP_{25}A$: syringopeptin 25A; SRE: syringomycin E; LDP: lipodepsipeptide; PLM: planar lipid membranes; SV: slow vacuolar (channel); PC: phosphatidylcholine; PE: phosphatidylethanolamine; PS: phosphatidylserine; LJP: liquid junction potential; R_a: access resistance; EDTA: ethylenediaminetetraacetic acid.

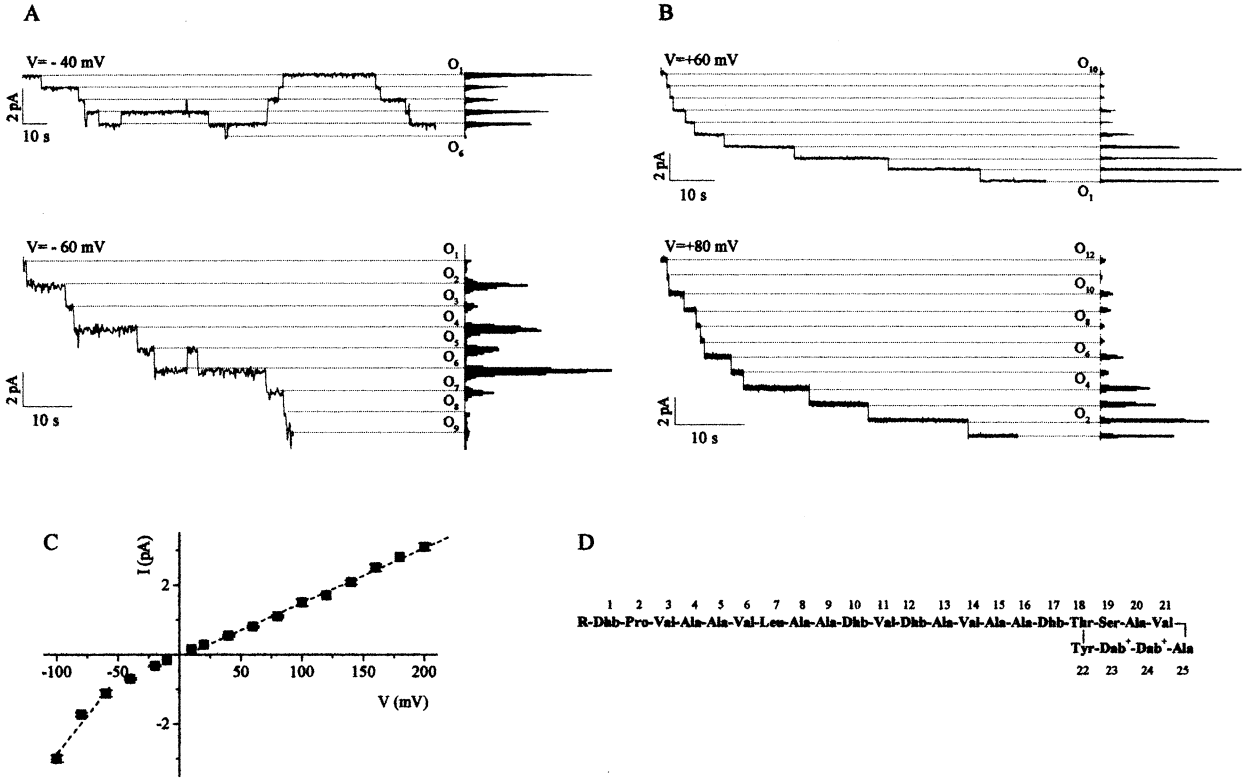

Fig. 1. Single-channel transitions of ion channels formed by $SP_{25}A$ in asolectin planar lipid bilayers. Panels *A* and *B*: representative traces, displaying single-channel transitions of $SP_{25}A$-induced current, in symmetrical solutions (Solution C) at the indicated voltages. As a result of the gating mechanism, in the initial portion of the records, channels open at negative voltages (panel *A*, traces at −40 and −60 mV) and close at positive voltages (panel *B*, traces at +60 and +80 mV). The different open levels (indicated by O_i, where i = 1, 2, ... *n* is the number of single channels simultaneously open) are identified by dashed lines. On the right, the occupation histograms of the corresponding levels are reported. Panel *C*: *I-V* characteristic of a single $SP_{25}A$ channel. Each current amplitude is derived from the current steps observed in experiments like those reported in the upper panels. The *I-V* curve is nonlinear, i.e., conductance at negative applied voltages (g_-) is larger than that at positive voltages (g_+). The two limiting slope conductances are (*dashed lines*) $g_- = 45 \pm 11$, pS, $g_+ = 15.6 \pm 0.3$ pS, providing $g_-/g_+ = 2.9 \pm 0.7$. Final $SP_{25}A$ concentration was 12.5 nM. A total of 200 single-channel transitions, taken from 2 different experiments, were analyzed. Panel *D*: Primary structure of $SP_{25}A$. Non-standard amino acids are: Dab, 2,4-diaminobutanoic acid and Dhb, 2,3-dehydro-2-aminobutyric acid; R: 3-hydroxydecanoyl.

thereby being involved in a variety of plant diseases. The production of LDPs, in particular $SP_{25}A$, during plant infection was recently demonstrated by an immunological approach (Fogliano et al., 1999).

It was recently shown that $SP_{25}A$ can form ion channels in planar lipid membranes (PLM) (Dalla Serra et al., 1999b). The ability to form transmembrane ion channels appears to be a common functional motif of all *P. syringae* LDPs (Hutchison, Tester & Gross, 1995; Feigin et al., 1996; Hutchison & Gross, 1997; Bender, Alarcon Chaidez & Gross, 1999; Agner et al., 2000a; Malev et al., 2000) as well as other similar cyclolipopeptide antibiotics from *Bacillus spp.* (Peypoux et al., 1986; Sheppard et al., 1991; Maget-Dana & Peypoux, 1994; Eshita et al., 1995; Maget-Dana & Ptak, 1995; Yakimov, Fredrickson & Timmis, 1996; Grau et al., 2000), and may provide the basis for understanding the mechanism of action of these molecules. Although the main target of $SP_{25}A$ and related LDPs is probably the plasma membrane of plant cells, several lines of evidence indicate that also intracellular membranes may be affected. This is suggested by: 1) the capacity of destabilizing and crossing the plasma membrane (Camoni et al., 1995), 2) the closure of leaf stomata induced by the toxin (Di Giorgio et al., 1996a) (which involves a redistribution of vacuolar ions and a decrease of the vacuolar volume (MacRobbie, 2000)), 3) the striking effects induced by the toxin on isolated mitochondria at submicromolar doses (Di Giorgio et al., 1996b). Actually, LDPs are in general active against a variety of membranes, though a marked dependence upon lipid composition has been observed (Julmanop et al., 1993; Camoni et al., 1995; Dalla Serra et al., 1999a).

Here we have used the plant vacuole, i.e., the intracellular storage organelle that occupies up to 90% of the cytoplasmic volume of plant cells, as a new model system for studying the mode of action and the channel-forming capacity of LDPs. The

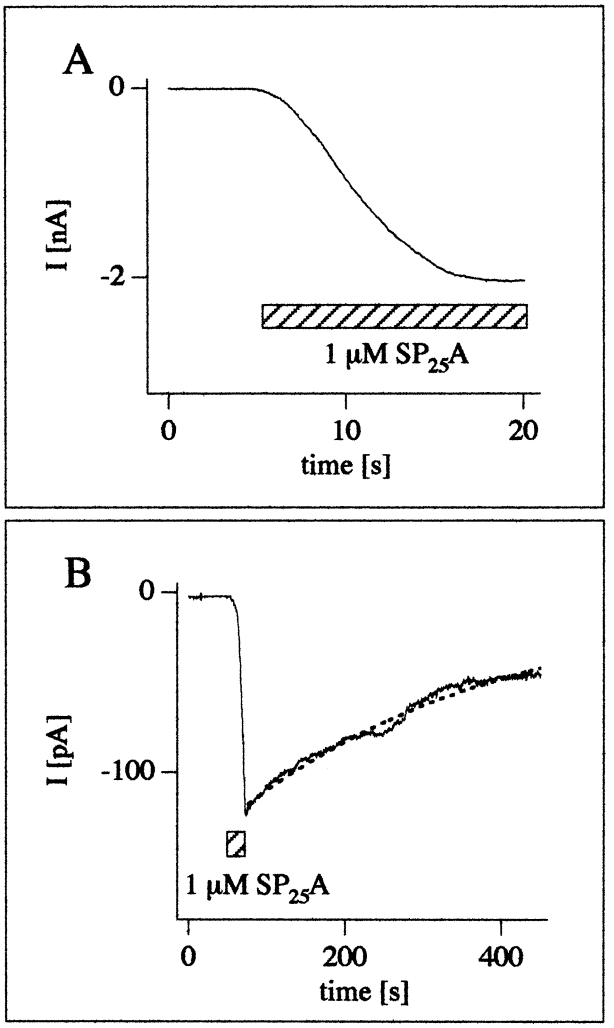

Fig. 2. $SP_{25}A$ increases the ionic permeability in sugar beet tonoplast. (*A*) Increase of the macroscopic current (downward deflection) induced by the fast perfusion of a whole-vacuole patch by a solution containing 1 μM $SP_{25}A$. The dashed bar indicates the application of $SP_{25}A$. Solution *A* was used both in the pipette and in the bath. Applied membrane potential was −50 mV. (*B*) Short perfusion of a cytoplasmic-side-out excised-patch with 1 μM $SP_{25}A$. The perfusion with the toxin was interrupted before reaching the current plateau. Soon after removing the toxin, a slow decrease of the ionic current is evident. Internal solution (in mM): KCl 200, $MgCl_2$ 2, $CaCl_2$ 1, Mes 10, pH 6.0. Bath solution: KCl 150 mM, Hepes 15 mM, pH 7.2 (adding KOH). Both solutions were supplemented with sorbitol up to the sugar beet osmolarity (i.e. 665 mOsm in that case). Applied membrane potential was −50 mV. The single decaying exponential (dashed curve) has a relaxation time, τ, of 332 ± 8 sec.

permeabilizing activity of $SP_{25}A$ on vacuolar membranes (tonoplasts) was studied with the patch-clamp technique. Compared to artificial membranes composed of pure lipids, the vacuole is a fully natural membrane that contains a variety of lipids (phospholipids, glycolipids and neutral lipids (Tavernier, Le Quoc & Le Quoc, 1993; Behzadipour et al., 1998)) as well as proteins that may act as regulators, or even receptors, for $SP_{25}A$. Therefore, $SP_{25}A$ action on this biologically complete membrane may differ significantly even from that on the synthetic counterparts. In addition, the tonoplast has considerable technical advantages with respect to other natural membranes, such as the easy isolation, the possibility of making fast and durable seals, and that of providing reliable control conditions measuring endogenous vacuolar channels (Gambale et al., 1996; Carpaneto, Cantù & Gambale, 1999; 2001).

Materials and Methods

Chemicals

$SP_{25}A$ was prepared and purified as previously described (Ballio et al., 1991). Its concentration in stock solutions was determined by amino-acid analysis and quantification by LC-MS as described (Monti et al., 2001). The lipid used in PLM experiments was soybean asolectin repurified according to Kagawa and Racker (1971) from a commercial product (Sigma, St. Louis, MO). According to previous analysis (Demel et al., 1991), it had the following composition: phosphatidylcholine, 24%; phosphatidylethanolamine, 39%; phosphatidylserine, 19%; phosphatidic acid, 6% phosphatidylinositol 1%; lyso derivatives 9%; other phospholipids 2%. Reagents were all the best grade available and were used without further purification.

Patch-Clamp Experiments

Sugar beet (*Beta vulgaris* L., kindly provided by Agra, Massalombarda, Italy, cv DURO) vacuoles were prepared and used as already described in Gambale et al. (1996). Briefly, they were extruded directly into the recording chamber by slicing the sugar beet root in standard bath solution (Solution A: KCl 150 mM, EDTA 1 mM, Mes 10 mM, pH 6.0, adjusted by KOH∼5 mM). Currents were recorded in the whole-vacuole or in the cytoplasmic-side-out excised-patch configurations. Applied voltages and currents were controlled and recorded with a List EPC7 patch-clamp amplifier (List-electronic, Darmstadt/Eberstadt, Germany) interfaced with an Instrutech AD/DA board (Instrutech, Elmont, N.Y.). Data analysis was done by home-made programs using IgorPro (Wavemetrics Inc., Lake Oswego, OR). The sign convention on endomembranes was adopted, i.e., the potential difference across the vacuolar membrane, V, is calculated as $V = V_{cytosol} - V_{vacuole}$ (Bertl et al., 1992). This convention implies that positive currents represent cations that flow out of the cytosol and enter the vacuole. If not otherwise specified in the text, the standard solution was Solution A for both the pipette and the bath. The osmotic pressure of the solutions was always adjusted to the same value of the sugar beet (between 600 and 680 mOsm) by adding appropriate concentrations of sorbitol. Osmolarities of ionic solutions and sugar beet were measured with a vapor pressure osmometer (Wescor Inc., Logan, UT). For the selectivity experiments, the bathing solution was either KCl 50 mM, EDTA 1 mM, Mes 10 mM, pH 6.0 adjusted by ∼5 mM KOH (called Solution B), or a variant of Solution A, in which 150 mM KCl was substituted with an equal concentration of KF, KNO_3 or Kgluconate (called KF, KNO_3 or Kgluconate solution, respectively). The bathing medium was changed by a fast perfusion system using up to five perfusion pipettes (with tip diameter around 30–35 μm); each pipette was filled with the suitable

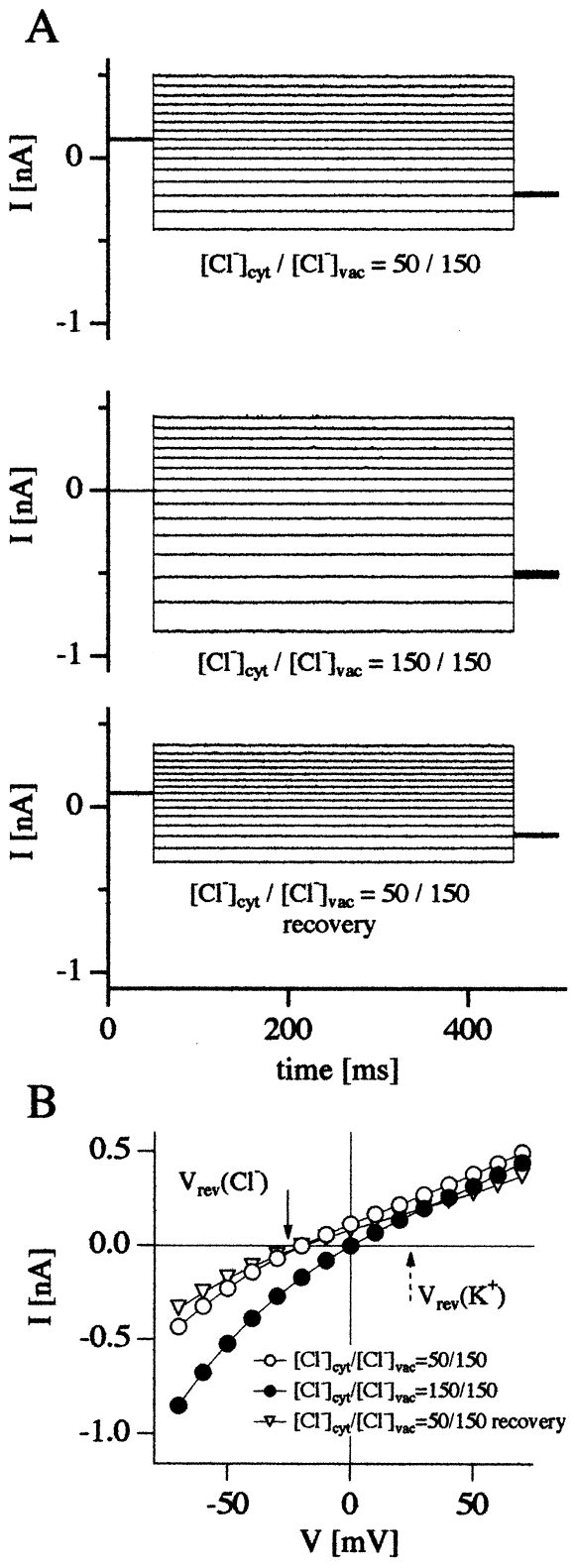

Fig. 3. Current-voltage characteristics of the $SP_{25}A$ channel. (*A*) After the application of 1 μM $SP_{25}A$ in the standard bath solution (for 20 sec), macroscopic currents were elicited by a series of voltage pulses ranging from −70 mV to +70 mV in 10-mV steps. Holding and tail potentials were at 0 and −50 mV, respectively. Cytoplasmic-side-out excised-patch was used. *Upper traces*: $SP_{25}A$-mediated currents in asymmetrical conditions; the pipette contained KCl 150 mM (Solution A), the bath contained KCl 50 mM (Solution B). The negative value of the zero-current voltage (*see* also panel *B*) indicates anionic selectivity of the $SP_{25}A$ channel. *Middle traces*: currents of the same vacuole in symmetric conditions. Both the pipette and the bath contained the standard Solution A. Zero-current now corresponds to zero applied voltage and a more marked inward rectification is evident. *Lower traces*: restoration of the asymmetrical conditions (as in the upper traces) moves the reversal voltage to the left (*see* Panel *B*). (*B*) Current-voltage characteristics derived from the traces in *A*. Open symbols represent the steady-state currents recorded in asymmetrical conditions (∇ is for the recovery experiment); filled symbols represent the current recorded in symmetrical condition. The current carried by endogenous channels (recorded in the same experiment, but before toxin application) was very low, less than 5 pA at −50 mV. The theoretical reversal voltages for chloride and potassium (indicated by the arrows) are −25.7 and +24.3 respectively. The reversal voltages in control and recovery asymmetrical conditions were −19.4 and −19.0 mV, respectively. V_{rev} in symmetrical conditions was 0.6 mV.

bath solution. Piezoelectric manipulators supported by hydraulic manipulators allowed to alternatively exchange the perfusing pipettes in front of the vacuole (which has a typical diameter of 10–20 μm). Similarly, the toxin was supplemented directly onto the patch through one of the perfusion pipettes filled with the standard bath solution plus 1 μM $SP_{25}A$. The contribution of the liquid junction potential (LJP) produced by solutions B, KF, KNO_3 or Kgluconate was estimated as follows. The solutions of the patch pipette and the bath were made KCl 3 M and solution A, respectively. Thereafter, the perfusion system was positioned with one of the five pipettes, containing the test solution, directly in front of the patch pipette and the corresponding voltage was measured. This voltage represents the LJP arising between the perfusing solution and the bath solution (Neher, 1992). We obtained the following values (in mV): solution A, 0; solution B, 0; KF solution, −2.8; KNO_3 solution, −1.3; Kgluconate solution, −8.1. These values were subtracted online during the recordings. To keep the bath solution clean, in the experiments for the determination of LJP or selectivity, the recording chamber was also slowly perfused with solution A via a gravity system. Experiments were performed at room temperature (≈25°C). The relative permeabilities were evaluated from the zero-current reversal voltage (V_{rev}) measured from the current-voltage (*I-V*) characteristic using the following modified Goldman-Hodgkin-Katz equation (Hille, 1992):

$$\frac{P_A}{P_{Cl}} = \frac{[Cl^-]_{vac}}{[A^-]_{cyt}} e^{\frac{FV_{rev}}{RT}} + \frac{P_K}{P_{Cl}} \frac{[K^+]_{cyt} e^{\frac{FV_{rev}}{RT}} - [K^+]_{vac}}{[A^-]_{cyt}} \quad (1)$$

where F, R and T have their usual meaning, $[A^-]_{cyt}$ is the anion activity in the cytosol; $[Cl^-]_{vac}$, the chloride activity in the vacuole; $[K^+]_{cyt}$ and $[K^+]_{vac}$ are the symmetrical potassium activities in the cytosol and in the vacuole; P_A, P_{Cl}, P_K are the anion, chloride and potassium permeabilities, respectively. V_{rev} is the reversal voltage measured in the presence of each anion. Activity coefficients were taken from Robinson and Stokes (1959) and Pitzer (1979). We used 0.741, 0.726, 0.744 and 0.756, respectively, for KF, KNO_3, KCl and NaCl. The activity coefficient of Kgluconate was assumed to be comparable to that of other potassium salts of organic anions bearing a carboxyl group (e.g., KHmalonate and KHsuccinate) and therefore estimated to be 0.72. The membrane capacity and the access resistance (R_a) of the vacuole were measured using the compensation circuitry of the patch-clamp amplifier (List EPC7). In whole-vacuole measurements, the applied voltage was corrected

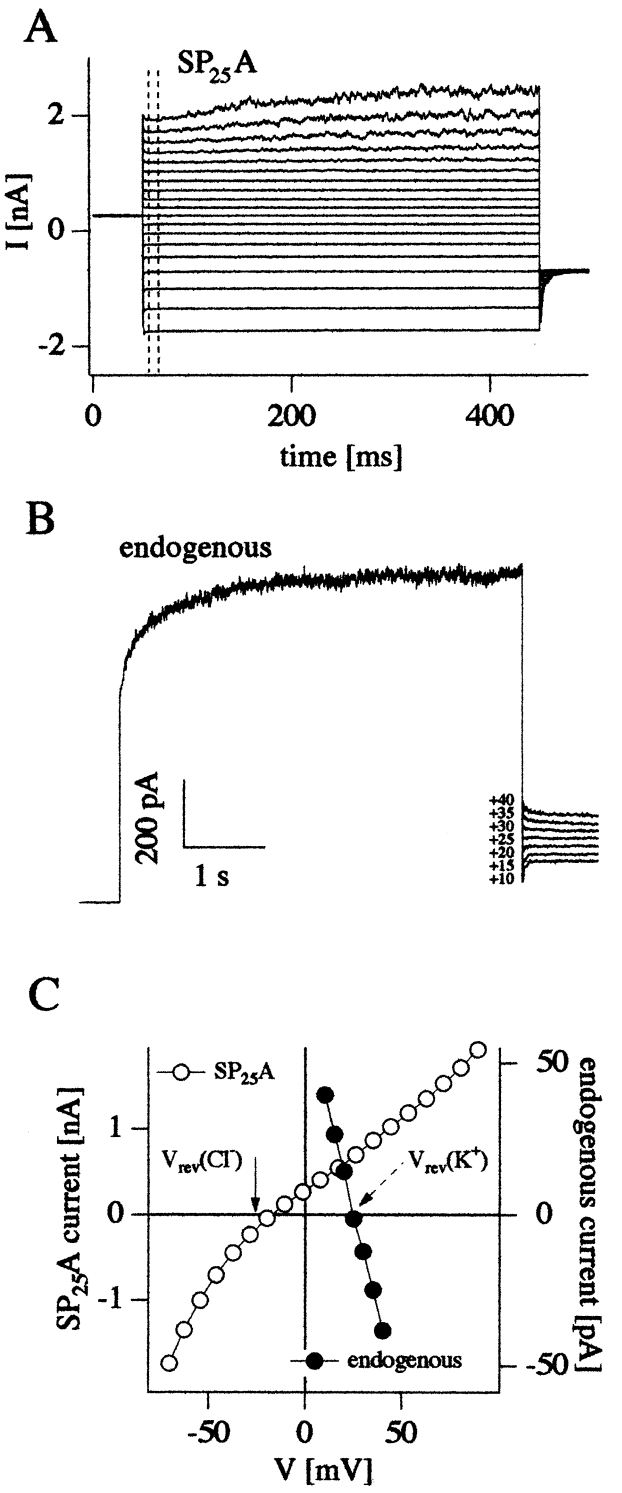

Fig. 4. Simultaneous recording of Slow Vacuolar (SV) endogenous currents and $SP_{25}A$ currents. (*A*) Whole-vacuole currents elicited by a series of voltage steps from −80 mV to +100 mV (in 10-mV increments); holding and tail potentials were 0 and −50 mV, respectively. The presence of the SV endogenous channel is evident from the time course at high positive applied potentials. Asymmetrical bath and pipette solutions (solution *B* and *A*, respectively). (*B*) Instantaneous tail currents elicited by a step voltage to +120 mV followed by tail voltages from +10 mV to +40 mV. Tail currents reverse at a voltage of +24.6 mV (right dashed arrow in panel *C*) within experimental error from the theoretical reversal voltage for potassium (+24.3 mV), indicating the cation selectivity of the SV channels. The current induced by the main voltage pulse is the average of 7 traces. (*C*) Open symbols: *I-V* characteristic of $SP_{25}A$ channels calculated as the average of the currents between the two dashed lines displayed in panel *A*. Applied voltage corrected for access resistance, R_a. The reversal voltage (−17.5 mV) is close to the theoretical reversal voltage for chloride (−25.7 mV, indicated by the left arrow). Tail currents of SV channels (shown in *B*) were fitted to the exponential function $A_0 + A_1 \exp(-t/\tau)$; filled symbols represent A_1 versus its corresponding tail voltage.

off-line for R_a when the estimated error was greater than 5 mV. Data were low-pass filtered with a four-pole Bessel filter set at frequencies between 0.1 and 5 kHz and sampled at a frequency from 2 to 5 times that of the low-pass filter for final storage. Upon reproduction, single-channel data were further filtered with a digital low-pass filter (provided by IgorPro) at a frequency of 5 or 10 Hz.

Planar Lipid Bilayer Experiments

Planar lipid bilayers were prepared by the apposition technique (Montal & Mueller, 1972) as already described (Dalla Serra et al., 1999b). Briefly, two monolayers were spread from a 6-mg/ml asolectin solution in *n*-hexane and apposed on the two sides of a hole (0.1 mm in diameter) in a 12-μm thick Teflon foil pretreated with *n*-hexadecane. Four ml of bathing solution (Solution C: NaCl 100 mM, Mes 10 mM, EDTA 1 mM at pH 6.0, adjusted by NaOH) were added on each side of the hole. Experiments were made at room temperature (≈25°C). $SP_{25}A$ was added on one side only (the cis side) and only to stable preformed bilayers. Typically, untreated membranes had a capacity of 100 pF and a conductance not exceeding 10 pS. Voltage-clamp experiments were performed with a Dagan 3900A patch clamp amplifier (Dagan Corporation, Minneapolis, MN). Membrane current was converted to voltage at 1 mV/pA, the signal was low-pass filtered at 1 kHz and stored on video cassettes via a PCM recorder (PCM-701ES from Sony, Tokyo, Japan) connected to a standard video recorder (JVC HR-D180E). For display and analysis the traces were low-pass filtered at 100 Hz, acquired on a personal computer and analyzed with the software package IgorPro. As in the patch-clamp experiments, the trans side was used as the reference. The current was therefore defined positive when cations flow into that compartment (upward deflections in the figures).

Statistics

Unless otherwise specified in the text, data are given as mean ± SD and are the results of at least three different experiments.

Results

As we have previously shown (Dalla Serra et al., 1999b), addition of the phytotoxic lipodepsipeptide $SP_{25}A$ to the solution bathing a PLM, promptly increases membrane permeability by producing step-like current transitions representative of ion channel formation (Fig. 1*A*). Compared to our previous results (Dalla Serra et al., 1999b), which were obtained

with membranes comprised of a mixture of synthetic lipids, i.e., phosphatidylcholine (PC), phosphatidylethanolamine (PE) and phosphatidylserine (PS) in a 2:2:1 ratio, here the use of asolectin, a natural plant lipid mixture, provided a lower voltage requirement for opening of the channels. In fact, $SP_{25}A$ channels open only when negative voltages are applied through the membrane, but quickly close when the voltage is reversed to positive values (a mechanism usually called 'voltage-dependent channel gating'). In this regard, much higher negative values (in the range of −140 mV) were required for opening in pure phospholipid compositions (Dalla Serra et al., 1999b) than in the present natural mixture (in the range of −40 to −60 mV, Fig. 1*A*). To the contrary, the single-channel conductance and the nonlinearity of the current-voltage (*I-V*) characteristic were almost unchanged. In fact, reporting single-channel currents observed at different voltages in an *I-V* curve (Fig. 1*C*), it is possible to extrapolate the limiting single-channel conductances for large positive and large negative voltages, called g_+ and g_- respectively. With asolectin PLMs, we calculated $g_+ = 15.6 \pm 0.3$ pS and $g_- = 45 \pm 11$ pS, which should be compared with those measured earlier in PC:PE:PS (2:2:1) PLMs, i.e., $g_+ = 26.0 \pm 0.5$ pS and $g_- = 57 \pm 3$ pS (Dalla Serra et al., 1999b). The *I-V* nonlinearity, which can be accounted by the conductance ratio g_-/g_+, was comparable in the two lipid systems: $g_-/g_+ = 2.9 \pm 0.7$ in asolectin and 2.2 ± 0.1 in PC:PE:PS PLMs.

As with synthetic model membranes, the application of 1 μM $SP_{25}A$ to sugar beet vacuoles (held in the whole-vacuole patch-clamp configuration) induces a significant increase in membrane permeability (Fig. 2*A*). Before the application of $SP_{25}A$, the current elicited in the tonoplast by a membrane potential of −50 mV is very low (less than 10 pA); as soon as the toxin perfuses the vacuole (dashed bar in Fig. 2*A*), the current increases and in some seconds it reaches a new stationary level. The fast perfusion procedure (*see* Material and Methods) allows us also to rapidly remove the toxin from the bathing solution and observe the following slow inactivation process that leads to the relaxation of the toxin-induced current (Fig. 2*B*). This decay (already described in Ziegler, Pavlovkin & Pokornj, 1984; Dalla Serra et al., 1999a; Agner et al., 2000b) can be fit to a single-exponential relaxation (dashed line in Fig. 2*B*) with a time constant, τ, of about 300 sec. This relatively slow rundown of the current allows the investigation of the biophysical properties of the channels formed by $SP_{25}A$ in external solutions that do not contain the toxin. As an example, the macroscopic currents elicited by different voltage steps after the transient application of 1 μM $SP_{25}A$ are shown in Fig. 3*A* in asymmetrical (upper and bottom panels) and symmetrical (middle panel) concentrations of KCl. These traces were obtained consecutively from the same vacuole (from top to bottom). In agreement with the slow decay of the current (Fig. 2*B*), the recovery of the currents when returning to the initial conditions is almost complete, with only a slight decrease within the 30 sec of the test (compare upper and bottom panels in Fig. 3*A*).

The current-voltage (*I-V*) characteristics obtained from the traces in Fig. 3*A* are given in Fig. 3*B* together with very low endogenous currents, recorded before the application of the toxin. The reversal membrane potential V_{rev}, derived from the *I-V* relationships in asymmetrical conditions, indicates that the $SP_{25}A$ channels are selective for chloride with respect to potassium with a permeability ratio, $P_{Cl}/P_K = 6.7 \pm 1.3$ (from 5 different vacuoles).

By decreasing the duration of toxin exposure and increasing the tonoplast surface (in the whole-vacuole configuration), it is possible to simultaneously record and distinguish the macroscopic currents carried either by the endogenous channels or by $SP_{25}A$-induced channels. In Fig. 4*A* macroscopic endogenous Slow Vacuolar (SV) currents and $SP_{25}A$-induced currents are represented, respectively, by the time-dependent component present at positive voltages and by the time-independent component present at all voltages (Colombo, Lado & Peres, 1987; Hedrich & Neher, 1987). Tail current experiments (Fig. 4*B*) confirm the cationic nature of the SV channel, as indicated by the good agreement between the estimated reversal voltage (filled symbols in Fig. 4*C*) and the theoretical K^+ reversal voltage (dashed arrow). On the other hand, the time-independent component of the currents, measured between the dashed lines in Fig. 4*A*, reveals the anionic preference of the $SP_{25}A$ pores, as demonstrated by the close vicinity between V_{rev} of the *I-V* characteristic (open symbols in Fig. 4*C*) and the theoretical reversal voltage for chloride (solid arrow). Therefore, instead of representing a drawback, the presence of endogenous vacuolar channels guarantees the functionality of the tonoplast, thus providing further evidence on the reliability of this model system.

To further investigate the selectivity properties of the $SP_{25}A$ channels, we substituted KCl in the standard bath solution with other potassium salts. Figure 5 shows an example of five consecutive current families recorded in the same vacuole perfused with bath solutions of different composition. Panel *A* displays the $SP_{25}A$ currents in control conditions (symmetrical standard solutions); panels *B*, *C* and *D* display the currents recorded after replacing the external KCl with KF, KNO_3 or Kgluconate, respectively. Panels *E* and *J*, instead, represent the recovery of the current when the vacuole was perfused again with KCl. A

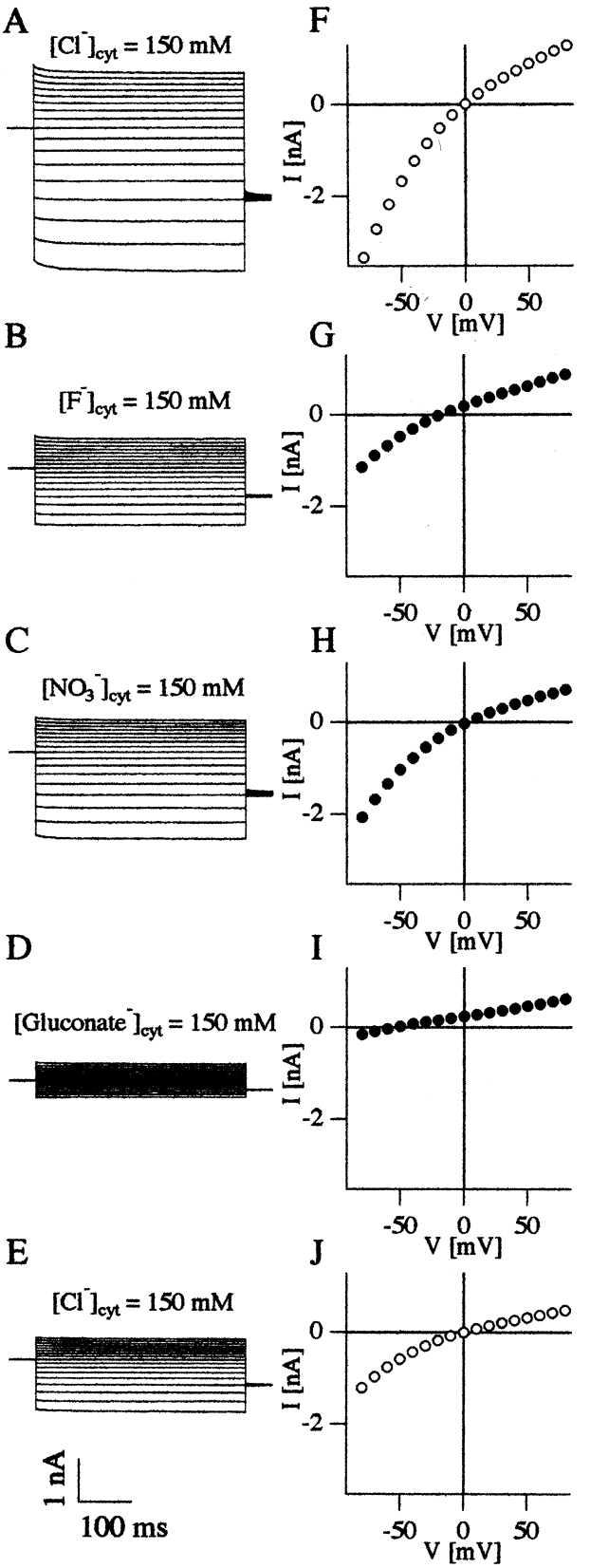

Fig. 5. Different anion permeabilities of the $SP_{25}A$ channel. (*A–E*) $SP_{25}A$ currents elicited by a series of voltage pulses from −80 to +80 mV in 10-mV steps from a 0 mV holding voltage. Tail voltage at −50 mV. In all panels, pipette solution was Solution A; bath solution was: (*A*) Cl^- 150 mM, (*B*) F^- 150 mM, (*C*) NO_3^- 150 mM, (*D*) gluconate$^-$ 150 mM, (*E*) Cl^- 150 mM. Other components of the bath solution as in Solution A. Data recorded from one single vacuole are shown in the same order they were recorded. Panel *E* represents the recovery of the current at the end of the experiment. (*F–J*) *I-V* characteristics of the traces in *A–E*. In *F*, the level of endogenous currents recorded before the incorporation of the toxin was less than ±11 pA at V = ±80 mV. The absence of any development of nonselective leak current was ascertained by reducing again the KCl concentration in the bath to 50 mM (solution B) and verifying that the reversal voltage shifted back to the value indicating the anion selectivity of the $SP_{25}A$ channel (*data not shown*).

Table 1. Relative permeability ratios of $SP_{25}A$

Anion	V_{rev} mV	Equivalent radius* Å	P_A/P_{Cl}
Cl^-	0	1.81	1
NO_3^- (4)	2.1 ± 0.4	1.99	1.16 ± 0.02
F^- (3)	−14.5 ± 1.6	1.33	0.50 ± 0.04
Gluconate$^-$ (3)	−48.4 ± 1.7	3.76	0.021 ± 0.018

Relative permeability ratios calculated according to a modified GHK equation (*see* Materials and Methods). V_{rev} is the reversal voltage measured after the substitution of 150 mM cytosolic chloride with the same concentration of the indicated anion. In column 1 the numbers in parentheses indicate the number of different vacuoles tested for each anion. Data in columns 2 and 4 are given as mean ± SE. *Equivalent radius from Smith et al. (1999).

comparison of the traces in panels *A* and *E* indicates a reduction of $SP_{25}A$ currents, likely dependent on the desorption/inactivation mechanism already discussed (Fig. 2*B*, *see* also Discussion).

Relative permeabilities evaluated from the reversal potentials measured from the *I-V* characteristics (as in Fig. 5*F–I*) using Eq. 1 (*see* Materials and Methods), are summarized in Table 1. The following selectivity profile for $SP_{25}A$ channels can be deduced: $NO_3^- \approx Cl^- > F^- >$ gluconate$^-$.

The macroscopic currents shown in Figs. 2–5 are mediated by discrete events, as evidenced by the fact that single $SP_{25}A$ channels can be recorded by incorporating few toxin molecules in small tonoplast patches. Some representative traces, at different membrane potentials, are shown in Fig. 6*A*. Single-channel transitions can also be resolved during the desorption/inactivation of the toxin when only a few pores remain open (Fig. 6*B*). The upper trace, obtained at −60 mV after the removal of the toxin from the bath solution, clearly shows (especially in the final part) such discrete closings. The bottom trace reports similar transitions at V = −80 mV. The analysis of the single-channel values at various membrane potentials is summarized in Fig. 7*A* where the conductance estimated by linear regression of the *I-V* characteristic gives $g_- = 35 \pm 7$ pS and

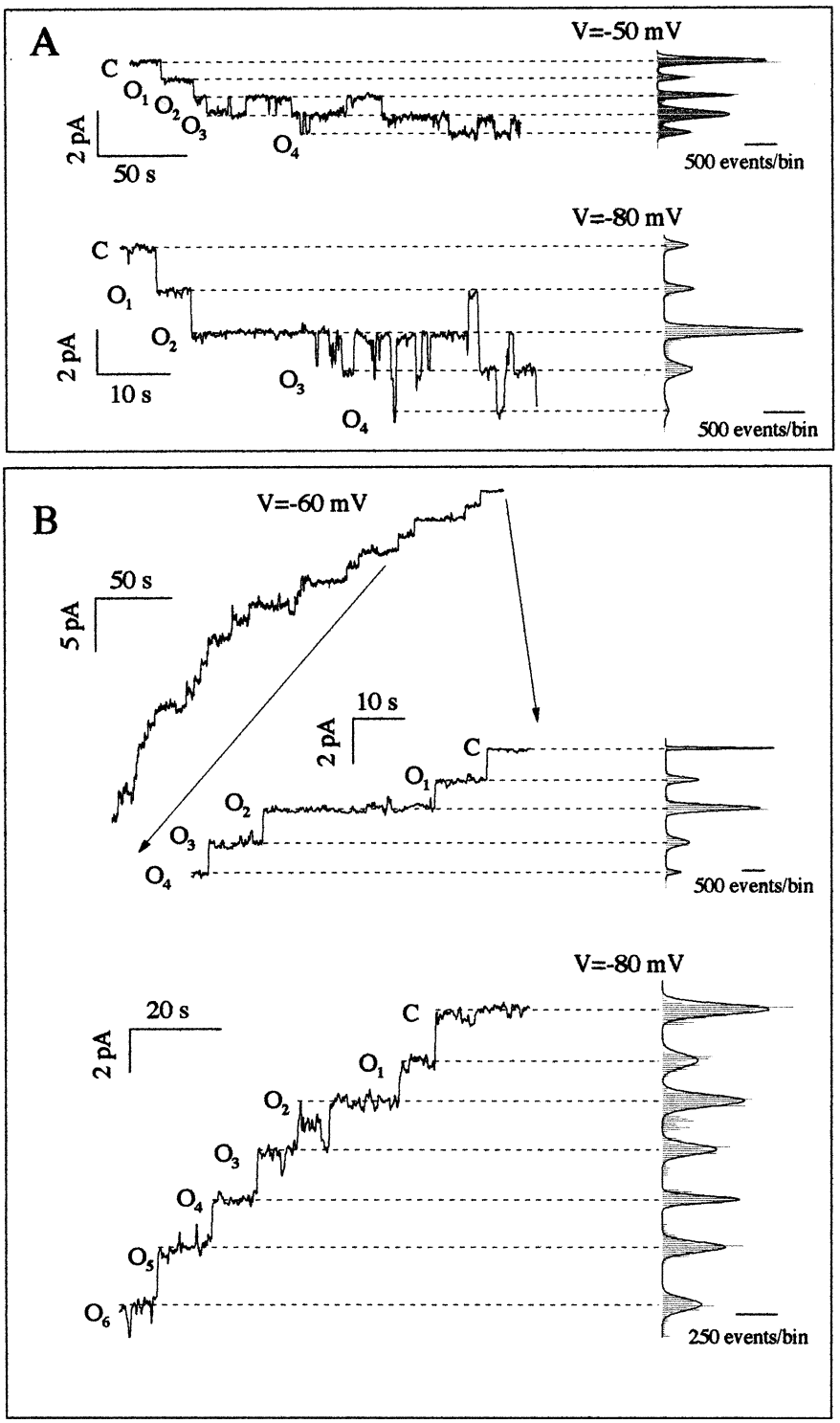

Fig. 6. Single-channel transitions of ion channels formed by $SP_{25}A$. (*A*) Representative single-channel transitions of $SP_{25}A$ toxin recorded at two different voltages (−50 mV upper trace and −80 mV bottom trace) in symmetrical standard solutions. The closed state (C) and the different open levels (O_i, i = 1, 2, 3 and 4) are indicated by dashed lines. Histograms to the right show the occupation time of the corresponding trace. The amplitudes of the bin at $V = -50$ mV and −80 mV are 0.05 and 0.1 pA, respectively. (*B*) *Upper trace*: desorption/inactivation of the toxin in the absence of $SP_{25}A$ in the bath solution. The magnification of the final part (comprised between the two arrows) reveals four single-channel closures. *Bottom trace*: similar single-channel transitions at $V = -80$ mV. On the right, occupation histograms of the corresponding traces; the amplitude of the bin is 0.1 pA at both voltages.

$g_+ = 10 \pm 3$ pS, only slightly smaller than those measured with asolectin membranes. The resulting rectification ratio, $g_-/g_+ = 3.5 \pm 1.3$, is consistent not only with that estimated from PLMs (around 3), but also with that determined from macroscopic vacuolar currents. In fact, if we call G_- and G_+ the conductance evaluated from tonoplast membranes containing many $SP_{25}A$ channels at negative and positive voltages, respectively (Fig. 7*B*), we get $G_-/G_+ = 3.4 \pm 0.7$ (4 different vacuoles). This suggests that rectification derives essentially from single-channel properties and not from the gating mechanism, implying a substantial independence of the gating from the applied voltage.

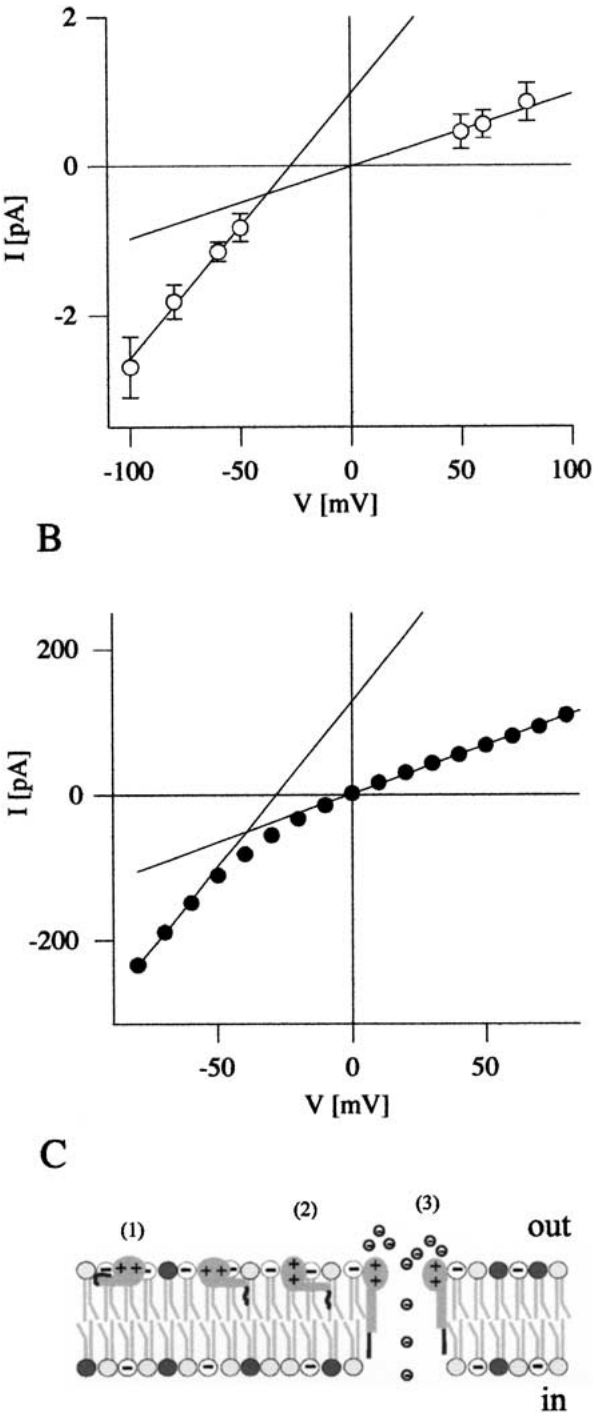

Fig. 7. The rectification property of the channels formed by $SP_{25}A$ depends on a different single-channel conductance at negative and positive voltages. (*A*) Single channel *I-V* characteristic. The continuous lines (representing the fit of the *I-V* curve at negative and positive voltages) gave the following conductance: $g_- = 35 \pm 7$ pS and $g_+ = 10 \pm 3$. A total of 480 single-channel transitions from 4 different vacuoles were measured. (*B*) Evaluation of G_- and G_+ from a typical *I-V* characteristic obtained from macroscopic recordings. The continuous lines represent the fit of the *I-V* characteristic at high negative and high positive voltages. (*C*) Schematic mechanism of pore formation (*see* Discussion for details). *In* and *out* indicate, respectively, the inside and the outside (cytoplasmic side) of the vacuole.

Discussion

The activity of *Pseudomonas* LDPs is thought to depend strictly on their ability to form transmembrane pores. However, though several in vitro and in vivo experiments have been performed in order to characterize the LDPs' mode of action, the molecular events occurring during plant tissue infection by *Pseudomonas* are still unclear. For example, there is already evidence that, besides the plasma membrane, $SP_{25}A$ may also act on the membranes of internal organelles. In fact, the capacity to physically damage plasma membrane integrity (Camoni et al., 1995), the decreased turgor induced by the toxin at the level of leaf stomata (Di Giorgio et al., 1996a) with the consequent release of vacuolar ions (MacRobbie, 2000), and the remarkable effects on isolated mitochondria (Di Giorgio et al., 1996b), suggest that also intracellular membranes may be a target for $SP_{25}A$. In this respect it is of interest that LDPs are considered virulence factors for pathogenic *Pseudomonas*; in fact, their production leads to an increased severity of disease while knock-out mutants producing only one LDP have reduced virulence, (Xu & Gross, 1988; Takemoto, 1992). It is possible that disrupting tonoplast integrity could be advantageous for the bacterium since it gets access to metabolites stored in the plant vacuole. Therefore, in this paper we have thoroughly investigated the interaction of $SP_{25}A$ with the membrane of the vacuole. Interestingly, we observed that micromolar concentrations of $SP_{25}A$ induced a significant increase of the tonoplast permeability at low physiological voltages (Fig. 2).

In contrast to results obtained with PLM made of pure phospholipid mixtures (PC:PE:PS 2:2:1 or PC:PS 4:1) where large negative voltages (≤ -140 mV) were necessary to gate toxin insertion (Dalla Serra et al., 1999b), no voltage-dependent gating was apparent in the plant vacuole. However, as in the vacuole membrane, also in PLM prepared with asolectin (a natural plant phospholipid mixture similar in composition to the tonoplast membrane (Tavernier, Le Quoc & Le Quoc, 1993; Behzadipour et al., 1998)) small voltages are sufficient to trigger pore opening (Fig. 1). This lipid dependence, also observed by others (Julmanop et al., 1993; Malev et al., 2001), suggests that lipids might participate in the $SP_{25}A$ gating mechanism. According to the above observations, the steps inducing the channel formation (Fig. 7*C*) could be the following: 1) partitioning of the folded LDP monomer into the membrane; 2) alignment of the unfolded hydrophobic part of the peptide with the lipid tails; 3) aggregation and formation of a barrel-stave pore. The anion selectivity of these pores correlated nicely with the molecular structure of the component LDP in view of the presence, at the pore entrance, of the positive charge of the cyclic peptide moiety that would attract anions and repel cations (*see* also below).

The transient application of the LDP used here has evidenced another feature of $SP_{25}A$ pores, i.e., a slow inactivation of the induced current after toxin removal (Fig. 2*B*). The time course of this decrease is well described by a single-exponential function. From our data we cannot discriminate between an irreversible inactivation of the $SP_{25}A$ channel within the membrane or the desorption of the toxin from the membrane phase. A slow desorption/inactivation of the toxin has been observed by several authors in different systems, although its basis remains unclear (*see* Ziegler, Pavlovkin & Pokornj, 1984; Dalla Serra et al., 1999a). Recently, Agner (2000b) has found a strong temperature dependence of the current decay, suggesting that it may be modulated by membrane fluidity. Several possibilities remain still open: peptide desorption from the membrane to the solution phase; a conformational transition of the membrane-bound peptide from an active to an inactive state; migration to a membrane compartment that does not influence membrane conductance (e.g., the annulus region surrounding the PLM or the omega region around the patch pipette). As far as the in vivo situation is concerned, it is likely that inactivation, if present, is compensated by de novo synthesis of peptide.

As in PLM, the $SP_{25}A$ channel in the tonoplast shows anion selectivity and inward rectifying properties (in symmetric KCl) that characterize both the macroscopic ($G_-/G_+ = 3.4 \pm 0.6$) and the single-channel level ($g_-/g_+ = 3.5 \pm 1.3$). This indicates that the rectification is due to a different single-channel conductance at negative and positive voltages rather than to a modification of single-channel open probability. It has been suggested (Dalla Serra et al., 1999b) that this nonlinearity may depend on the asymmetric distribution of the positive charges that are located in the hydrophilic part of the molecule (the cyclic ring) and thus conceivably remain located at the cytoplasmic side of the pore. By accumulating anions at the cytoplasmic entrance of the pore, such asymmetric distribution of charges may cause a larger anion current when negative voltages are applied on that side. This would increase anion currents entering the vacuole. Consistently, when the poorly permeant anion gluconate$^-$ replaces chloride on the cytosolic side, a strong reduction of the current at negative voltages is observed, which leads to a nearly linear *I-V* characteristic (Fig. 5).

The fact that fluoride, which has a great energy of hydration (−472 kJ/mol), can easily permeate through the $SP_{25}A$ channel, suggests that the pore is water-filled. This possibility was also proposed by Dalla Serra et al. (1999b) on the basis of an almost linear relationship between the conductance of $SP_{25}A$ and the conductivity of the bathing solution at different salt concentrations. Consistently with the osmotic protection of erythrocytes suggesting a pore radius ≈0.9 nm (Dalla Serra et al., 1999a), or of calcein release from vesicles, suggesting a pore radius >0.55 nm (Dalla Serra et al., 1999a), gluconate$^-$ (radius = 0.376 nm) is able to permeate the channel, albeit to a reduced extent. It was reported (Smith et al., 1999) that gluconate$^-$ has a great energy of hydration (−376 kJ/mol) due to the locally high charge density resulting from its non-uniform charge distribution. If gluconate$^-$ permeates through the channel with its hydration shell, the effective radius of hydrated gluconate$^-$ could increase from 0.376 up to 0.66 nm (Hille, 1992).

As in PLM, also in plant vacuoles $SP_{25}A$ channels are stable for several seconds (Fig. 6). The presence of slightly different conductance levels (bottom trace of Fig. 6*B*) (probably due to the presence of substates) is also worth noting. Substates were previously observed in PLM both with $SP_{25}A$ (Dalla Serra et al., 1999b) and with the parent toxin SRE (Kaulin et al., 1998).

One important difference between vacuoles and PLM is the concentration of $SP_{25}A$ that had to be used to observe single channels, which was in the range of 1 μM and 12.5 nM, respectively (Figs. 6 and 1). However, these values are justified by the difference in the amount of exposed membrane area in the two systems. On the basis of typical membrane capacities of ∼100 pF and of ∼0.1 pF for PLMs and excised patches, respectively, a PLM has an area around 1000 times larger than that of an excised vacuolar patch. Since diffusion of peptides in the plane of the membrane is very fast, the probability that absorbed peptide monomers come together to form an oligomeric channel onto one single membrane depends on their total number rather than on their actual density. Therefore, assuming a constant partition coefficient, an excised vacuolar patch absorbs the same number of peptides at a toxin concentration around 1000 times larger than a PLM. We verified that a toxin concentration 100 times larger in vacuoles with respect to PLM is sufficient to observe single-channel transitions.

Finally, we wish to stress that the simultaneous presence of both endogenous and $SP_{25}A$-induced channels (Fig. 4) is important to verify the integrity of the vacuolar membrane and the reliability of the measurements.

In conclusion, this paper describes the interaction of $SP_{25}A$ with a real plant membrane, demonstrating that it can form pores by a mechanism similar to that observed in artificial bilayers; the physiological relevance of these data should be evaluated in the light of the effective amount of LDPs produced during infection (Fogliano et al., 1999).

The technical assistance provided by G. Gaggero and D. Magliozzi was highly appreciated. We thank S. De Robertis for English-language assistance. This work was financially supported by the Italian Consiglio Nazionale delle Ricerche (CNR), in part through

a Progetto Finalizzato CNR Biotecnologie by the Istituto Trentino di Cultura (ITC) and by PAT Fondo Progetti (Project AgriBio). Syringopeptin 25A was kindly supplied by Prof. A. Ballio to whom this paper is dedicated.

References

Agner, G., Kaulin, Y., Gurnev, P., Szabo, Z, Schagina, L., Takemoto, J., Blasko, K. 2000a. Membrane-permeabilizing activities of cyclic lipodepsipeptides, syringopeptin 22A and syringomycin E from *Pseudomonas syringae* pv. *syringae* in human red blood cells and in bilayer lipid membranes. *Bioelectrochemistry* **52:**161–167

Agner, G., Kaulin, Y., Schagina, L., Takemoto, J., Blasko, K. 2000b. Effect of temperature on the formation and inactivation of syringomycin E pores in human red blood cells and bimolecular lipid membranes. *Biochim. Biophys. Acta* **1466:**79–86

Ballio, A., Barra, D., Bossa, F., Collina, A., Grgurina, I., Marino, G., Moneti, G., Paci, M., Pucci, P., Segre, A., Simmaco, M. 1991. Syringopeptins, new phytotoxic lipodepsipeptides of *Pseudomonas syringae* pv. *syringae*. *FEBS lett*. **291:**109–112

Ballio, A., Bossa, F., Collina, A., Gallo, M., Iacobellis, N.S., Paci, M., Pucci, P., Scaloni, A., Segre, A., Sommaco, M. 1990. Structure of syringotoxin, a bioactive metabolite of *Pseudomonas syringae* pv. *syringae*. *FEBS Lett*. **269:**77–380

Ballio, A., Bossa, F., Di Giorgio, D., Di Nola, A., Manetti, C., Paci, M., Scaloni, A., Segre, A. 1995. Solution conformation of the *Pseudomonas syringae* pv. *syringae* phytotoxic lipodepsipeptide syringopeptin 25-A. Two-dimensional NMR, distance geometry and molecular dynamics. *Eur. J. Biochem*. **234:**747–758

Behzadipour, M., Ratajczak, R., Faist, K., Pawlitschek, P., Trémolières, A., Kluge, M. 1998. Phenotypic adaptation of tonoplast fluidity to growth temperature in the CAM plant *Kalanchoe daigremontiana* Ham. et Per. is accompanied by changes in the membrane phospholipid and protein composition. *J. Membrane Biol*. **166:**61–70

Bender, C., Alarcon Chaidez, F., Gross, D. 1999. *Pseudomonas syringae* phytotoxins: mode of action, regulation, and biosynthesis by peptide and polyketide synthetases. *Microbiol. Mol. Biol. Rev*. **63:**266–292

Bertl, A., Blumwald, E, Coronado, R., Eisenben, R., Firlay, G., Gradmann, D., Hille, B., Kohler, K., Koll, H.A., MacRobbie, E, Meissner, G., Miller, C., Neher, E, Palade, P. 1992. Electrical measurements on endomembranes. *Science* **258:**873–874

Bradbury, J. 1986. *Guide to plant pathogenic bacteria*. Farnham Royal CAB International Mycological Institute, England

Camoni, L., Di Giorgio, D., Marra, M., Aducci, P., Ballio, A. 1995. *Pseudomonas syringae* pv. *syringae* phytotoxins reversibly inhibit the plasma membrane H^+-ATPase and disrupt unilamellar liposomes. *Biochem. Biophys. Res. Commun*. **214:**118–124

Carpaneto, A., Cantù, A.M., Gambale, F. 1999. Redox agents regulate ion channel activity in vacuoles from higher plant cells. *FEBS Lett*. **442:**129–132

Carpaneto, A., Cantù, A.M., Gambale, F. 2001. Effects of cytoplasmic Mg^{2+} on slowly activating channels in isolated vacuoles of *Beta vulgaris*. *Planta* **213:**457–468

Colombo, R., Lado, P., Peres, A. 1987. A hyperpolarization-activated K^+ current in isolated vacuoles of *Acer pseudoplatanus*. *In*: Plant vacuoles. B. Marin, editor. pp. 51–56. Plenum Publisher, New York

Dalla Serra, M., Fagiuoli, G., Nordera, P., Bernhart, I., Della Volpe, C., Di Giorgio, D., Ballio, A., Menestrina, G. 1999a. The interaction of lipodepsipeptide toxins from *Pseudomonas syringae* pv. *syringae* with biological and model membranes: a comparison of syringotoxin, syringomycin and syringopeptins. *Mol. Plant - Microbe Interact*. **12:**391–400

Dalla Serra, M., Nordera, P., Bernhart, I., Di Giorgio, D., Ballio, A., Menestrina, G. 1999b. Conductive properties and gating of channels formed by syringopeptin 25-A, a bioactive lipodepsipeptide from *Pseudomonas syringae* pv. *syringae*, in planar lipid membranes. *Mol. Plant - Microbe Interact*. **12:**401–409

Demel, R., Schiavo, G., de Kruijff, B., Montecucco, C. 1991. Lipid interaction of diphtheria toxin and mutants. A study with phospholipid and protein monolayers. *Eur. J. Biochem*. **197:**481–486

Di Giorgio, D., Camoni, L., Ballio, A. 1994. Toxins of *Pseudomonas syringae* pv. s*yringae* affect H^+-transport across the plasma membrane of maize. *Physiol. Plant*. **91:**741–746.

Di Giorgio, D., Camoni, L., Mott, K., Takemoto, J., Ballio, A. 1996a. Syringopeptins, *Pseudomonas syringae* pv. *syringae* phytotoxins, resemble syringomycin in closing stomato. *Plant Pathol*. **45:**564–571

Di Giorgio, D., Lavermicocca, P., Marchiafava, C., Camoni, L., Surico, G., Ballio, A. 1996b. Effect of syringomycin-E and syringopeptins on isolated plant mitochondria. *Physiol. Mol. Plant Pathol*. **48:**325–334.

Eshita, S., Roberto, N., Beale, J., Mamiya, B., Workman, R. 1995. Bacillomycin Lc, a new antibiotic of the iturin group: isolation, structures and antifungal activities of the congeners. *J. Antibiotics* **48:**1240–1247

Feigin, A., Takemoto, J., Wangspa, R., Teeter, J., Brand, J. 1996. Properties of voltage-gated ion channels formed by syringomycin E in planar lipid bilayers. *J. Membrane Biol*. **149:**41–47

Fogliano, V., Gallo, M., Vinale, F., Ritieni, A., Randazzo, G., Greco, M., Lops, R., Graniti, A. 1999. Immunological detection of syringopeptins produced by *Pseudomonas syringae* pv. *lachrymans*. *Physiol. Mol. Plant Pathol*. **55:**255–261

Gambale, F., Bregante, M., Stragapede, F., Cantù, A.M. 1996. Ionic channels of the sugar beet tonoplast are regulated by a multi-ion single-file permeation mechanism. *Arch. Membrane Biol*. **154:**69–79

Grau, A., Ortiz, A., de Godos, A, Gomez-Fernandez, J. 2000. A biophysical study of the interaction of the lipopeptide antibiotic iturin A with aqueous phospholipid bilayers. *Arch. Biochem. Biophys*. **377:**315–323

Han, F., Mortishire-Smith, R., Rainey, P., Williams, D. 1992. Structure of the White-Line-Inducing Principle isolated from *Pseudomonas reactans*. *Acta Crystallographica* **C48:**1965–1968

Hedrich, R., Neher, E. 1987. Cytoplasmic calcium regulates voltage-dependent ion channels in plant vacuoles. *Nature* **329:**833–835

Hille, B. 1992. *Ionic channels of excitable membranes*. Sinauer Assoc. Inc, Sunderland, MA

Hutchison, M., Gross, D. 1997. Lipopeptide phytotoxins produced by *Pseudomonas syringae* pv. *syringae*: Comparison of the biosurfactant and ion channel-forming activities of syringopeptin and syringomycin. *Mol. Plant-Microbe Interact*. **10:**347–354

Hutchison, M., Tester, M., Gross, D. 1995. Role of biosurfactant and ion channel-forming activities of syringomycin in transmembrane ion flux: a model for the mechanism of action in the plant-pathogen interaction. *Mol. Plant - Microbe Interact*. **8:**610–620

Iacobellis, N., Lavermicocca, P., Grgurina, I., Simmaco, M., Ballio, A. 1992. Phytotoxic properties of *Pseudomonas syringae* pv. *syringae* toxin. *Physiol. Mol. Plant Pathol*. **40:**107–116

Isogai, A., Iguchi, H., Nakayama, J., Kusai, A., Takemoto, J., Suzuki, A. 1995. Structural analysis of new syringopeptins by tandem mass spectrometry. *Biosci. Biotech. Biochem*. **59:**1374–1376

Julmanop, C., Takano, Y., Takemoto, J., Miyakawa, T. 1993. Protection by sterols against the cytotoxicity of syringomicin in the yeast *Saccharomyces cerevisiae*. *J. Gen. Microbiol*. **139:**2323–2327

Kagawa, Y., Racker, E. 1971. Partial resolution of the enzymes catalyzing oxidative phosphorilation. XXV. Reconstitution of vesicles catalyzing inorganic phosphorus-32-adenosine triphosphate exchange. *J. Biol. Chem.* **246:**5477–5487

Kaulin, Y., Schagina, L., Bezrukov, S., Malev, V., Feigin, A., Takemoto, J., Teeter, J., Brand, J. 1998. Cluster organization of ion channels formed by the antibiotic syringomycin E in bilayer lipid membranes. *Biophys. J.* **74:**2918–25

MacRobbie, E.A.C. 2000. ABA activates multiple Ca^{2+} fluxes in stomatal guard cells, triggering vacuolar K^+ (Rb^+) release. *Proc. Natl. Acad. Sci. USA* **24:**12361–12368

Maget-Dana, R., Peypoux, F. 1994. Iturins, a special class of pore-forming lipopeptides: biological and physicochemical properties. *Toxicology* **87:**151–174

Maget-Dana, R., Ptak, M. 1995. Interactions of surfactins with membrane models. *Biophys. J.* **68:**1937–1943.

Malev, V., Kaulin, Y., Bezrukov, S., Gurnev, P., Takemoto, J., Schagina, L. 2000. Kinetics of opening-closure of syringomycin E channels formed in lipid bilayers. *Biol. Membrany* **17:**653–665

Malev, V., Schagina, L., Takemoto, J., Nestorovich, E., Bezrukov, S. 2001. Gating and conductance of syringomycin E channels as manifestations of an asymmetrical channel structure. *Biophys. J.* **80:**132a

Montal, M., Mueller, P. 1972. Formation of bimolecular membranes from lipid monolayers and a study of their electrical properties. *Proc. Natl. Acad. Sci. USA* **69:**3561–3566

Monti, M., Gallo, M., Ferracane, R., Borrelli, C., Ritieni, A., Greco, M., Graniti, A., Fogliano, V. 2001. Analysis of bacterial lipodepsipeptides by MALDI-TOF and electrospray mass spectrometry. *Rapid Comm. Mass Spec.* **15:**623–628

Mortishire-Smith, R., Nutkins, J., Packman, L., Brodey, C., Rainey, P., Johnstone, K., Williams, D. 1991. Determination of the structure of an extracellular peptide produced by the mushroom saprophytic *Pseudomonas reactans*. *Tetrahedron* **47:**3645–3654

Neher, E. 1992. Correction for liquid junction potentials in patch clamp experiments. *Methods Enzymol.* **207:**123–131

Peypoux, F., Pommier, M., Marion, D., Ptak, M, Das, C., Michel, G. 1986. Revised structure of mycosubtilin, a peptidolipid antibiotic from *Bacillus subtilis*. *J. Antibiotics* **39:**636–641

Pitzer, K.S. 1979. Theory: ion interaction approach. *In*: Activity coefficients in electrolyte solutions. R. Pytkovicy, editor. pp. 157–208. CRC Press, Boca Raton Florida

Robinson, R.A., Stokes, R.H. 1959. *Electrolyte solutions*. Butterworths Scientific Publications, London

Sheppard, J., Jumarie, C., Cooper, D., Laprade, R. 1991. Ionic channels induced by surfactin in planar lipid bilayer membranes. *Biochim. Biophys. Acta* **1064:**13–23

Smith, S., Steinle, E., Meyerhoff, M., Dawson, D. 1999. Cystic fibrosis transmembrane conductance regulator: physical basis for lyotropic anion selectively patterns. *J. Gen. Physiol.* **114:**799–817

Takemoto, J. 1992. Bacterial phytotoxins syringomycin and its interaction with host membranes. *In*: Molecular signals in plant-microbe communications. D. Verma, editor. pp. 247–260. CRC Press, Boca Raton

Tavernier, E., Le Quoc, D., Le Quoc, K. 1993. Lipid composition of vacuolar membrane of *Acer pseudoplatanus* cultured cells. *Biochim. Biophys. Acta* **167:**242–247

Xu, G., Gross, D. 1988. Evaluation of the role of syringomycin in plant pathogenesis by using Tn5 mutants of *Pseudomonas syringae* pv. *syringae* defective in syringomycin production. *Appl. Environ. Microbiol.* **54:**1345–1353

Yakimov, M., Fredrickson, H., Timmis, K. 1996. Effect of hetero geneity of hydrophobic moieties on surface activity of lychenysin A, a lipopeptide biosurfactant from *Bacillus licheniformis* BAS50. *Biotechnol. Appl. Biochem.* **23:**13–18

Ziegler, W., Pavlovkin, J., Pokornj, J. 1984. Effect of syringotoxin on the permeability of bilayer lipid membranes. *Biologia* **39:**693–699